

Ternary Mutual Diffusion Coefficients from Error-Function Dispersion Profiles: Aqueous Solutions of Triton X-100 Micelles + Poly(ethylene glycol)

Helga M. Halvorsen, Elzbieta Wygnal, Michael R. MacIver, and Derek G. Leaist*

Department of Chemistry, University of Western Ontario, London, Ontario, Canada N6A 5B7

Taylor dispersion has gained widespread popularity for measuring diffusion in liquids. The usual procedure is to inject small volumes of solution containing solute at concentration $\bar{c} + \Delta c$ into carrier streams of composition \bar{c} . Binary mutual diffusion coefficients D are evaluated from the Gaussian distribution of the dispersed solute measured at the outlet of a long capillary tube. As a result of strong dilution of the injected solute with the carrier solution, obtaining favorable signal-to-noise ratios for the measured profiles can require unacceptably large Δc values for solutions with strongly composition-dependent diffusion coefficients or broad dispersion profiles produced by slowly diffusing solutes. For these systems, D can be reliably evaluated from error-function profiles generated by changing the solution flowing into dispersion tube from composition $\bar{c} - (\Delta c/2)$ to $\bar{c} + (\Delta c/2)$. There are no dilution factors, so Δc can be orders of magnitude smaller than the values employed in conventional pulse-injection techniques. In the present study, the error-function dispersion technique is extended to measure coupled diffusion in three-component solutions using small Δc initial conditions. A least-squares procedure is developed to calculate ternary mutual D_{ik} coefficients from profiles generated by changing the solution flowing into a dispersion tube from composition $\bar{c}_1 - (\Delta c_1/2)$ and $\bar{c}_2 - (\Delta c_2/2)$ to $\bar{c}_1 + (\Delta c_1/2)$ and $\bar{c}_2 + (\Delta c_2/2)$. D_{ik} coefficients are measured for aqueous solutions of Triton X-100 + poly(ethylene glycol) at 25 °C to study the interactions between nonionic micelles and polymers.

Introduction

Taylor dispersion^{1–4} is used in many laboratories to measure mutual diffusion (chemical interdiffusion) in liquids.^{5–15} The usual procedure is to inject a small volume of solution containing solute at concentration $\bar{c} + \Delta c$ into a laminar carrier stream of composition \bar{c} . As the injected sample flows through a long capillary tube, radial diffusion and convection along the tube axis shape the initial δ concentration pulse into a Gaussian profile. Binary mutual diffusion coefficients (D) are calculated from the broadened distribution of the dispersed sample measured at the tube outlet. Extensions of this technique have been used to measure ternary^{16–18} and quaternary^{19,20} mutual diffusion coefficients (D_{ik}) for multicomponent solutions. These results include cross-coefficients D_{ik} ($i \neq k$) describing the coupled fluxes of solutes driven by concentration gradients in other solutes (information not available from light-scattering or NMR diffusion measurements). The dispersion of samples tagged with isotopes, although less frequently employed, can be used to measure self-diffusion in pure liquids and intradiffusion in multicomponent solutions of uniform chemical composition.²¹

Taylor experiments are convenient in practice because the injection of the solution samples and the measurement of the dispersion profiles can be automated using commercially available HPLC equipment. Calibration with solutions that have known diffusion coefficients is not required, and a variety of detection methods are available including differential refractometry, UV/visible absorbance, conductivity, and, more recently, mass spectrometry.²² Errors from unwanted convection—always

a concern in macroscopic-gradient diffusion experiments—are eliminated by confining the flowing solution within narrow-bore capillary tubing (i.d. < 1 mm).²³ This feature is important for multicomponent solutions because coupled diffusion in these systems can produce gravitational instabilities in free-diffusion boundaries,²⁴ even if the lower solution is initially denser than the upper solution.

The solution samples injected into Taylor dispersion tubes are very strongly diluted with the carrier stream, especially for slowly diffusing solutes that produce broad profiles. To obtain favorable signal-to-baseline-noise ratios for the measured dispersion profiles, the initial concentration differences are typically in the (0.01 to 0.10) mol·dm⁻³ range. Concentration differences of this magnitude can be unacceptably large for systems with strongly composition-dependent diffusion coefficients, such as dilute electrolytes²⁵ ($dD/dc \rightarrow -\infty$ as $c \rightarrow 0$), solutions near critical mixing points,^{1,26} and strongly associating solutes, including surfactant solutions in the region of the critical micelle concentration (cmc).^{27,28} For these systems D changes significantly and nonlinearly with concentration across the dispersed samples. As the injected samples move along the dispersion tube, moreover, dilution with the carrier solution causes the average concentration of diffusing solute to change continuously from $\bar{c} + (\Delta c/2)$ at time $t = 0$ to \bar{c} as $t \rightarrow \infty$.

These considerations prompted the development of “moving-boundary” dispersion experiments²⁹ for systems with slowly diffusing solutes or highly variable diffusion coefficients. In these modified Taylor experiments, Gaussian profiles produced by dispersing δ concentration pulses are replaced by error-function concentration profiles generated from step-function initial conditions easily arranged in practice by switching the solution flowing into the dispersion tube from a solution of composition $\bar{c} - (\Delta c/2)$ to a solution of composition

* Corresponding author address: Department of Chemistry, St. Francis Xavier University, P.O. Box 5000, Antigonish, Nova Scotia, Canada B2G 2W5. Telephone: (902)867-5372. Fax: (902)867-2414. E-mail: dleaist@stfx.ca.

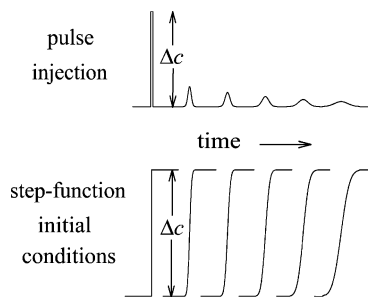


Figure 1. Time evolution of dispersion profiles. Top: Gaussian profiles generated by pulse injection of a small volume of solution of composition $\bar{c} + \Delta c$ into a carrier solution of composition \bar{c} . Dilution with the carrier solution strongly reduces the peak amplitude. Bottom: Error-function dispersion profiles (no dilution factors) generated using step-function initial conditions produced by changing the solution flowing into the dispersion tube from composition $\bar{c} - (\Delta c/2)$ to $\bar{c} + (\Delta c/2)$.

$\bar{c} + (\Delta c/2)$. There are no dilution factors in error-function dispersion experiments, as illustrated schematically in Figure 1. Also, the average concentration of the diffusing solute (\bar{c}) remains constant as error-function dispersion profiles move along the dispersion tube. For these reasons the concentration differences employed in error-function dispersion experiments can be orders of magnitude smaller than the typical Δc values used in conventional pulse-injection Taylor experiments, allowing, for example, the measurement of binary mutual diffusion coefficients for aqueous solutions of the surfactant Triton X-100 in the cmc region where D plunges by a factor of 3^{29} over a narrow concentration interval of about $0.0003 \text{ mol}\cdot\text{dm}^{-3}$. In another error-function dispersion study, the Boltzmann–Mantano transformation¹⁹ was used to measure concentration-dependent diffusion coefficients $D(c)$ over the concentration interval from to $\bar{c} - (\Delta c/2)$ to $\bar{c} + (\Delta c/2)$ in single experimental runs.

Many diffusion processes of scientific and technical interest involve the coupled diffusion of solutes in multicomponent solutions. The purpose of the present study is to extend error-function dispersion experiments from binary to ternary solutions in order to measure the coupled diffusion of two solutes using small ∇c initial conditions. In the notation used here, ternary mutual diffusion coefficient^{1,2} D_{ik} gives the molar flux J_i of solute i produced by the gradient ∇c_k in the molar concentration of solute k :

$$J_1 = -D_{11}\nabla c_1 - D_{12}\nabla c_2 \quad (1)$$

$$J_2 = -D_{21}\nabla c_1 - D_{22}\nabla c_2 \quad (2)$$

Expressions are derived in this paper for the ternary error-function dispersion profiles generated by changing the solution flowing into a dispersion tube from composition $\bar{c}_1 - (\Delta c_1/2)$ and $\bar{c}_2 - (\Delta c_2/2)$ to $\bar{c}_1 + (\Delta c_1/2)$ and $\bar{c}_2 + (\Delta c_2/2)$ at time $t = 0$. A least-squares procedure is developed to calculate the D_{ik} coefficients from the ternary profiles measured at the tube outlet.

For dilute solutions of non-interacting solutes, main coefficients D_{11} and D_{22} are identical to the binary diffusion coefficients of the respective solutes. Also, cross-coefficients D_{12} and D_{21} are negligibly small. To test the proposed analysis of ternary error-function profiles along these lines, D_{ik} coefficients are reported here for dilute aqueous solutions of mannitol (1) + glycine (2). Coefficients D_{11} and D_{22} are compared with accurate ($\approx 0.2\%$) binary mutual diffusion coefficients for aqueous mannitol³⁰ and glycine³¹ measured previously by Gouy interferometry.

Error-function dispersion profiles are also used to measure ternary mutual diffusion coefficients for aqueous solutions of Triton X-100 + poly(ethylene glycol) (PEG). This system was chosen to investigate the interaction between fluxes of nonionic Triton X-100 micelles and PEG polymers. In a recent study,³² PEG concentration gradients were reported to drive surprisingly large coupled fluxes of ionic sodium dodecyl sulfate (NaDS) micelles. For example, a gradient in PEG3400 (PEG, average molecular mass of $3400 \text{ g}\cdot\text{mol}^{-1}$) produced a coupled flow of about 20 mol of NaDS per mole of diffusing PEG3400. A possible explanation for this strongly coupled diffusion was developed based on the solubilization of PEG segments in NaDS micelles, the subsequent reduction of the charge density on the micelles, and the release of bound Na^+ counterions. The electric field generated to slow down the diffusing Na^+ ions to maintain electroneutrality was suggested to pull along substantial coupled fluxes of the anionic NaDS micelles together with the diffusing PEG. If this electrostatic mechanism is correct, then coupled diffusion in the nonionic Triton X-100 + PEG solutions studied here might be significantly weaker.

Experimental Section

Materials. Mannitol and glycine were BDH AnalaR products (purity > 99 %). PEG fractions of average molecular mass (400, 2000, and 4600) $\text{g}\cdot\text{mol}^{-1}$ were supplied by Aldrich. Triton X-100, the condensation product $(\text{CH}_3)_3\text{CCH}_2\text{C}(\text{CH}_3)_2\text{C}_6\text{H}_4\text{-O}(\text{CH}_2\text{CH}_2\text{O})_n\text{H}$ of ethylene oxide and an octyl phenol with $n = 9.5 \pm 0.5$, was obtained from Sigma. Solutions were prepared in calibrated volumetric flasks using distilled, deionized water.

Equipment. A peristaltic metering pump (Gilson model MP4) maintained a steady laminar flow of solution through a Teflon capillary tube (length 3000 cm, internal radius $r = 0.0385_5 \text{ cm}$, coiled in the form of a 70 cm diameter helix). The solution flowing into the dispersion tube was changed to a different solution using a two-way Teflon switching valve (Rheodyne model 5301) at the pump inlet. Dispersion profiles at the tube outlet were measured by a differential refractometer HPLC detector (Agilent model 1100). The detector output voltage $V(t)$ was measured by a computer-controlled digital voltmeter (Hewlett-Packard model 3478A). A 2 bar backpressure regulator connected to the refractometer outlet line minimized bubble formation. Flow rates were adjusted to give nominal retention times (t_R) of $1.5 \times 10^4 \text{ s}$. The pump, solutions, switching valve, and dispersion tube were held at $(25.00 \pm 0.05) \text{ }^\circ\text{C}$ in an air thermostat.

Binary Error-Function Dispersion Profiles. Step-function initial conditions arranged by switching the composition of the flowing solution from $\bar{c} - (\Delta c/2)$ to $\bar{c} + (\Delta c/2)$ at time $t = 0$ in a binary dispersion experiment produces the radially averaged concentration profile^{29,33}

$$c(t) - \bar{c} = \frac{\Delta c}{2} \text{erf}\left(\sqrt{\frac{12D}{t}} \frac{t - t_R}{r}\right) \quad (3)$$

at the tube outlet. The error function $\text{erf}(y)$ is

$$\text{erf}(y) = \frac{2}{\sqrt{\pi}} \int_0^y \exp(-\phi^2) d\phi \quad (4)$$

Changes in the refractometer voltage are accurately proportional to changes in solute concentration c :

$$V(t) - V(t_R) = k(\text{dn/dc})[c(t) - \bar{c}] \quad (5)$$

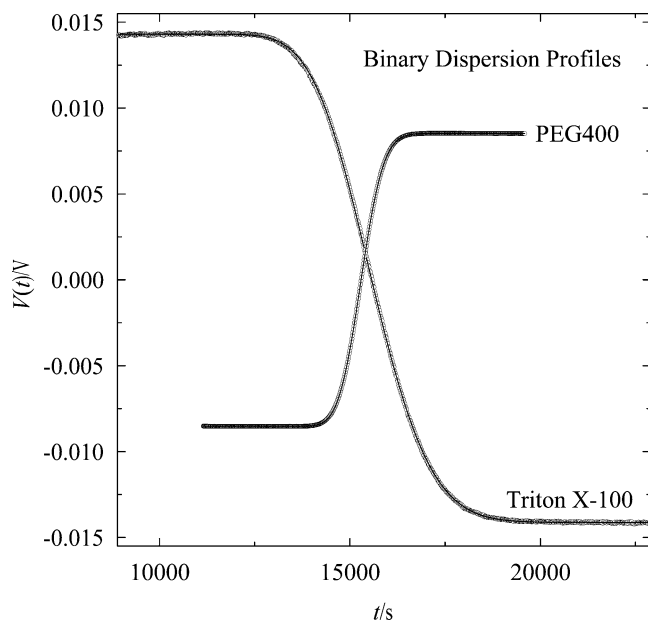


Figure 2. Measured and fitted binary error-function dispersion profiles for aqueous Triton X-100 ($\bar{c} = 5.00$ and $\Delta c = -1.00$ mmol·dm⁻³) and PEG400 ($\bar{c} = 5.00$ mmol·dm⁻³, $\Delta c = 1.00$ mmol·dm⁻³): ○, measured refractometer voltages; —, fitted refractometer voltages (eq 6).

n is the refractive index of the solution and $k = dV/dn$ is the detector sensitivity. Combining eqs 3 and 5 and adding the terms $B_0 + B_1t$ to allow for small linear drifts in the detector signal encountered in practice leads to the working expression

$$V(t) = B_0 + B_1t + \frac{\Delta V}{2} \operatorname{erf}\left(\sqrt{\frac{12D}{t}} \frac{t - t_R}{r}\right) \quad (6)$$

for the detector voltage. The step voltage difference is $\Delta V = k (dn/dc) \Delta c$.

A few runs were made for binary aqueous Triton X-100 or PEG solutions. The dispersion profiles were analyzed by fitting eq 6 to the detector voltages, treating D , t_R , B_0 , B_1 , and ΔV as adjustable least-squares parameters. The Triton X-100 and PEG profiles were accurately fitted by eq 6, as illustrated in Figure 2. These check runs indicated that the Triton X-100 and PEG samples had sufficiently small polydispersities to be treated as single diffusing components for the purpose of the present study. Four to six binary profiles measured for each average concentration \bar{c} gave the average D values listed in Table 1. The initial concentration differences were typically ± 1.00 mmol·dm⁻³. Smaller Δc values gave identical D values within the precision of the measurements.

As an additional check, conventional pulse-injection Taylor dispersion was used to measure binary diffusion coefficients for 0.0100 mol·dm⁻³ carrier solutions of the Triton X-100 and PEG samples for comparison with the error-function dispersion measurements. The two sets of results are listed in Table 1. Acceptable agreement is obtained, generally within the precision of the measurements. However, the Triton X-100 diffusion coefficients reported in an earlier error-function dispersion study ($(0.077$ to $0.080) \times 10^{-5}$ cm²·s⁻¹) are consistently higher than the values (0.060 to $0.067) \times 10^{-5}$ cm²·s⁻¹) reported here. We suspect, but cannot prove, that the sample of Triton X-100 used in the previous study had a lower average molecular weight.

Ternary Error-Function Dispersion Profiles. Ternary error-function profiles are generated by changing the solution flowing into the dispersion tube from a solution of composition $\bar{c}_1 -$

$(\Delta c_1/2)$ and $\bar{c}_2 - (\Delta c_2/2)$ to a solution of composition $\bar{c}_1 + (\Delta c_1/2)$ and $\bar{c}_2 + (\Delta c_2/2)$ at time $t = 0$. The expressions for the resulting ternary concentration profiles at the tube outlet

$$c_i(t) - \bar{c}_i = \sum_{p=1}^2 \sum_{q=1}^2 B_{ip} A_{pq} \frac{\Delta c_q}{2} \operatorname{erf}\left(\sqrt{\frac{12D_p}{t}} \frac{t - t_R}{r}\right) \quad (7)$$

are linear combinations^{17,18} of the functions used to represent binary error-function concentration profiles (eq 3). D_1 and D_2 are the eigenvalues of the matrix \mathbf{D} of ternary D_{ik} coefficients. The columns of the matrix of A_{ik} coefficients are eigenvectors of \mathbf{D} and matrix \mathbf{B} is the inverse of \mathbf{A} .

Using R_i to denote $\partial n/\partial c_i$, the detector voltage in a ternary dispersion experiment is

$$V(t) - V(t_R) = k[R_1(c_1(t) - \bar{c}_1) + R_2(c_2(t) - \bar{c}_2)] \quad (8)$$

Substituting eq 7 into eq 8 gives the cumbersome expression

$$V(t) - V(t_R) = k \sum_{i=1}^2 \sum_{p=1}^2 \sum_{q=1}^2 R_i B_{ip} A_{pq} \frac{\Delta c_q}{2} \operatorname{erf}\left(\sqrt{\frac{12D_p}{t}} \frac{t - t_R}{r}\right) \quad (9)$$

for $V(t)$, which can be simplified considerably by using

$$\frac{\Delta V}{2} = k \sum_{i=1}^2 \sum_{p=1}^2 \sum_{q=1}^2 R_i B_{ip} A_{pq} \Delta c_q = \frac{k}{2} (R_1 \Delta c_1 + R_2 \Delta c_2) \quad (10)$$

to define the normalized coefficients:

$$W_1 = \frac{\sum_{i=1}^2 \sum_{q=1}^2 R_i B_{i1} A_{1q} \Delta c_q}{(R_1 \Delta c_1 + R_2 \Delta c_2)/2} \quad (11)$$

$$W_2 = 1 - W_1 \quad (12)$$

and rewriting eq 10 as

$$V(t) - V(t_R) = \frac{\Delta V}{2} \left[W_1 \operatorname{erf}\left(\sqrt{\frac{12D_1}{t}} \frac{t - t_R}{r}\right) + W_2 \operatorname{erf}\left(\sqrt{\frac{12D_2}{t}} \frac{t - t_R}{r}\right) \right] \quad (13)$$

Equation 11 shows that W_1 is a linear function of the fraction of the initial refractive index difference produced by the concentration difference in component 1

$$\alpha_1 = \frac{R_1 \Delta c_1}{R_1 \Delta c_1 + R_2 \Delta c_2} \quad (14)$$

and therefore

$$W_1 = a + b\alpha_1 \quad (15)$$

$$W_2 = 1 - a - b\alpha_1 \quad (16)$$

where a and b are constants for dispersion profiles measured at average composition \bar{c}_1 and \bar{c}_2 .

Table 1. Binary Diffusion Coefficients for Aqueous Triton X-100, PEG400, PEG2000, and PEG4600 Solutions at 25 °C and Mean Solute Concentrations \bar{c}^a

Triton X-100		PEG400		PEG2000		PEG4600	
$\bar{c}/(\text{mmol}\cdot\text{dm}^{-3})$	$D/(10^{-5}\text{ cm}^2\cdot\text{s}^{-1})$	$\bar{c}/(\text{mmol}\cdot\text{dm}^{-3})$	$D/(10^{-5}\text{ cm}^2\cdot\text{s}^{-1})$	$\bar{c}/(\text{mmol}\cdot\text{dm}^{-3})$	$D/(10^{-5}\text{ cm}^2\cdot\text{s}^{-1})$	$\bar{c}/(\text{mmol}\cdot\text{dm}^{-3})$	$D/(10^{-5}\text{ cm}^2\cdot\text{s}^{-1})$
5.00	0.0672 (0.0008)	5.00	0.443 (0.003)	5.00	0.198 (0.001)	5.00	0.162 (0.002)
10.00	0.0665 (0.0012)	10.00	0.438 (0.002)	10.00	0.197 (0.002)	10.00	0.164 (0.003)
10.00	0.0645 ^b (0.0022)	10.00	0.444 ^b (0.002)	10.00	0.198 ^b (0.004)	10.00	0.157 ^b (0.005)
20.00	0.0638 (0.0020)						
30.00	0.0624 (0.0018)						
40.00	0.0595 (0.0012)						

^a Two standard deviations in parentheses. ^b Evaluated from Gaussian dispersion profiles produced by pulse injection.

Substituting eqs 15 and 16 into eq 13 and adding the terms $B_0 + B_1t$ to allow for small linear drifts in the detector signal provides to the fitting equation

$$V(t) = B_0 + B_1t + \frac{\Delta V}{2} \left[(a + b\alpha_1) \operatorname{erf} \left(\sqrt{\frac{12D_1}{t}} \frac{t - t_R}{r} \right) + (1 - a - b\alpha_1) \operatorname{erf} \left(\sqrt{\frac{12D_2}{t}} \frac{t - t_R}{r} \right) \right] \quad (17)$$

for ternary error-function profiles.

Ternary dispersion profiles are generally represented by two superimposed pseudo-binary error functions in D_1 and D_2 . For the particular initial conditions satisfying $a + b\alpha_1^{(1)} = W_1^{(1)} = 1$; however, eq 17 shows that the error function in D_2 vanishes. In this case the concentrations differences $\alpha_1^{(1)}/R_1$ and $(1 - \alpha_1^{(1)})/R_2$ provide an eigenvector of the matrix of D_{ik} coefficients with eigenvalue D_1 . Similarly, the error function in D_1 vanishes for initial conditions $a + b\alpha_1^{(2)} = W_1 = 0$ and $\alpha_1^{(2)}/R_1$. $(1 - \alpha_1^{(2)})/R_2$ is therefore an eigenvector with eigenvalue D_2 . Using values of eigenvalues and eigenvectors, the matrix of ternary D_{ik} coefficients is readily constructed by a similarity transform, giving

$$D_{11} = D_1 + \frac{a(1 - a - b)}{b}(D_1 - D_2) \quad (18)$$

$$D_{12} = \frac{R_2}{R_1} \frac{a(1 - a)}{b}(D_1 - D_2) \quad (19)$$

$$D_{21} = \frac{R_1(a + b)}{R_2} \frac{(1 - a - b)}{b}(D_2 - D_1) \quad (20)$$

$$D_{22} = D_2 + \frac{a(1 - a - b)}{b}(D_2 - D_1) \quad (21)$$

The D_{ik} coefficients reported in the present study were evaluated by fitting eq 17 to two or more profiles measured at the same average solution composition. B_0 , B_1 , ΔV , and t_R were used as adjustable least-squares parameters together with a , b , D_1 , and D_2 . The ratio R_2/R_1 required to evaluate α_1 , and the cross-coefficients D_{12} and D_{21} were evaluated by fitting the values of ΔV for each set of profiles to the linear equation

$$\Delta V = k(R_1\Delta c_1 + R_2\Delta c_2) \quad (22)$$

treating (kR_1) and (kR_2) as adjustable parameters and using $R_2/R_1 = (kR_2)/(kR_1)$.

Results and Discussion

Aqueous Mannitol (1) + Glycine (2) Solutions. The proposed analysis of ternary error-function dispersion profiles was tested

by measuring D_{ik} coefficients for dilute aqueous solutions of mannitol (1) + glycine (2) at the mean carrier-stream composition $\bar{c}_1 = 5.00$ and $\bar{c}_2 = 5.00$ mmol·dm⁻³ at 25 °C. The D_{ik} coefficients were evaluated by fitting eq 17 to profiles generated using initial concentrations differences in mannitol ($\Delta c_1 = \pm 1.00$ mmol·dm⁻³, $\Delta c_2 = 0.00$) or glycine ($\Delta c_1 = 0.00$, $\Delta c_2 = \pm 1.00$ mol·dm⁻³). Five different pairs of profiles were used to calculate the average D_{ik} coefficients listed in Table 2. Consistent with the diffusion properties of dilute solutions of nonionic nonassociating solutes, cross-coefficients D_{12} and D_{21} are zero within the precision of the measurements. In addition, main coefficients D_{11} and D_{22} are in good agreement ($\approx 2\%$) with accurate binary diffusion coefficients of aqueous mannitol and glycine measured previously by Gouy interferometry.

Aqueous Triton X-100 (1) + PEG (2) Solutions. Ternary error-function profiles for this system were measured at mean Triton X-100 concentrations from (5.00 to 40.0) mmol·dm⁻³ and mean PEG concentrations of (5.00 or 10.0) mmol·dm⁻³. The average D_{ik} coefficients determined from 4 to 6 replicate sets of profiles at each composition are listed in Tables 3 to 5 for solutions of Triton X-100 with added PEG400, PEG2000, or PEG4600, respectively. Figure 3 illustrates the close agreement (within $\approx 0.2\%$ of ΔV) obtained for the measured and fitted profiles.

To check the ternary error function analysis, D_{ik} coefficients at the composition 10.0 mmol·dm⁻³ Triton X-100 + 10.0 mmol·dm⁻³ PEG2000 were also measured by the pulse-injection dispersion technique. In these experiments 20 mm³ samples of solution containing 10.0 mmol·dm⁻³ excess Triton X-100 or PEG2000 were injected into 10.0 mmol·dm⁻³ Triton X-100 + 10.0 mmol·dm⁻³ PEG2000 carrier solutions. The resulting Gaussian profiles were analyzed by using the least-squares fitting procedure described in ref 17. The average D_{ik} coefficients evaluated from replicate pulse-injection experiments are listed in Table 4 for comparison with the coefficients from the error-function profiles. Acceptable agreement is obtained, within $(0.003 \text{ to } 0.008) \times 10^{-5} \text{ cm}^2\cdot\text{s}^{-1}$. The error-function results are evidently more precise. We attribute this result to the relatively slow diffusion of Triton X-100, which produces very broad dispersion profiles ($\approx 10^4$ s). Precise measurement of broad Gaussian profiles is challenging³⁴ because the peak amplitudes are small and drifts in HPLC detector baseline signals over a period of several hours can be troublesome.

Main coefficients D_{11} and D_{22} give the molar fluxes of the Triton X-100 (1) and PEG (2) components driven by their own concentration gradients. At the compositions used in the present study, added Triton X-100 produces relatively minor changes in D_{22} for PEG400, whereas the values of D_{22} for PEG2000 and PEG4600 generally drop as the concentration of Triton X-100 is raised. Similarly, added PEG leads to a decrease in D_{11} . The heaviest PEG used in the present study, PEG4600 (degree of polymerization ≈ 100), causes a relatively large

Table 2. Ternary Diffusion Coefficients for Aqueous Mannitol (1) + Glycine (2) Solutions at 25 °C and Mean Solute Concentrations \bar{c}_1 and \bar{c}_2^a

\bar{c}_1 mmol·dm ⁻³	\bar{c}_2 mmol·dm ⁻³	D_{11} 10 ⁻⁵ cm ² ·s ⁻¹	D_{12} 10 ⁻⁵ cm ² ·s ⁻¹	D_{21} 10 ⁻⁵ cm ² ·s ⁻¹	D_{22} 10 ⁻⁵ cm ² ·s ⁻¹
5.00	0.00	0.650 (0.005)			
5.00	0.00	0.6560 ^b			
0.00	5.00				1.071 (0.009)
0.00	5.00				1.060 ^c
5.00	5.00	0.66 (0.01)	-0.01 (0.01)	0.005 (0.007)	1.08 (0.02)

^a Two standard deviations in parentheses. ^b Gouy binary D value for aqueous mannitol interpolated from ref 30. ^c Gouy binary D value for aqueous glycine interpolated from ref 31.

Table 3. Ternary Diffusion Coefficients for Aqueous Triton X-100 (1) + PEG400 (2) Solutions at 25 °C and Mean Solute Concentrations \bar{c}_1 and \bar{c}_2^a

\bar{c}_1 mmol·dm ⁻³	\bar{c}_2 mmol·dm ⁻³	D_{11} 10 ⁻⁵ cm ² ·s ⁻¹	D_{12} 10 ⁻⁵ cm ² ·s ⁻¹	D_{21} 10 ⁻⁵ cm ² ·s ⁻¹	D_{22} 10 ⁻⁵ cm ² ·s ⁻¹
5.00	5.00	0.068 (0.002)	0.002 (0.002)	0.013 (0.003)	0.45 (0.02)
5.00	10.00	0.068 (0.002)	0.011 (0.003)	0.013 (0.002)	0.44 (0.02)
10.00	5.00	0.065 (0.001)	0.004 (0.003)	0.029 (0.014)	0.44 (0.01)
10.00	10.00	0.063 (0.002)	0.014 (0.002)	0.018 (0.008)	0.45 (0.02)
20.00	10.00	0.057 (0.001)	0.025 (0.003)	0.013 (0.003)	0.40 (0.02)
40.00	10.00	0.055 (0.002)	0.014 (0.002)	0.013 (0.005)	0.43 (0.02)

^a Two standard deviations in parentheses. molar refractive index ratio $R_2/R_1 = 0.601$.

Table 4. Ternary Diffusion Coefficients for Aqueous Triton X-100 (1) + PEG2000 (2) Solutions at 25 °C and Mean Solute Concentrations \bar{c}_1 and \bar{c}_2^a

\bar{c}_1 mmol·dm ⁻³	\bar{c}_2 mmol·dm ⁻³	D_{11} 10 ⁻⁵ cm ² ·s ⁻¹	D_{12} 10 ⁻⁵ cm ² ·s ⁻¹	D_{21} 10 ⁻⁵ cm ² ·s ⁻¹	D_{22} 10 ⁻⁵ cm ² ·s ⁻¹
5.00	5.00	0.061 (0.001)	0.010 (0.001)	0.003 (0.001)	0.201 (0.001)
5.00	10.00	0.055 (0.001)	0.011 (0.003)	0.000 (0.002)	0.201 (0.001)
10.00	5.00	0.058 (0.002)	0.004 (0.006)	0.010 (0.001)	0.199 (0.002)
10.00	10.00	0.053 (0.002)	0.012 (0.002)	0.003 (0.002)	0.200 (0.004)
		0.050 ^b (0.004)	0.004 ^b (0.003)	0.007 ^b (0.003)	0.203 ^b (0.008)
20.00	10.00	0.052 (0.002)	0.064 (0.003)	0.006 (0.001)	0.190 (0.002)
40.00	10.00	0.052 (0.001)	0.127 (0.004)	0.007 (0.002)	0.178 (0.004)

^a Two standard deviations in parentheses. Molar refractive index ratio $R_2/R_1 = 2.91$. ^b Evaluated from Gaussian dispersion profiles produced by pulse injection.

Table 5. Ternary Diffusion Coefficients for Aqueous Triton X-100 (1) + PEG4600 (2) Solutions at 25 °C and Mean Solute Concentrations \bar{c}_1 and \bar{c}_2^a

\bar{c}_1 mmol·dm ⁻³	\bar{c}_2 mmol·dm ⁻³	D_{11} 10 ⁻⁵ cm ² ·s ⁻¹	D_{12} 10 ⁻⁵ cm ² ·s ⁻¹	D_{21} 10 ⁻⁵ cm ² ·s ⁻¹	D_{22} 10 ⁻⁵ cm ² ·s ⁻¹
5.00	5.00	0.054 (0.005)	-0.01 (0.01)	0.0006 (0.0008)	0.183 (0.001)
5.00	10.00	0.035 (0.006)	0.03 (0.02)	0.0022 (0.0010)	0.180 (0.003)
10.00	5.00	0.050 (0.002)	-0.01 (0.02)	0.0023 (0.0008)	0.185 (0.006)
10.00	10.00	0.031 (0.003)	0.01 (0.01)	0.0057 (0.0004)	0.155 (0.002)
20.00	10.00	0.030 (0.002)	0.06 (0.01)	0.0048 (0.0002)	0.165 (0.002)
40.00	10.00	0.036 (0.003)	0.30 (0.03)	0.0026 (0.0003)	0.139 (0.003)

^a Two standard deviations in parentheses. Molar refractive index increment ratio $R_2/R_1 = 6.73$.

(up to ≈ 50 %) decrease in D_{11} (see Table 5). Qualitatively, this behavior is consistent with previous reports^{35,36} that PEG segments bind to Triton X-100 micelles. PEG-micelle association would increase the effective micelle size and friction coefficient. Longer PEG chains, moreover, can simultaneously bind to different micelles, forming transient networks of cross-linked micelles which would further slow their diffusion.

Cross-coefficient D_{21} gives the coupled flux of PEG produced by a Triton X-100 concentration gradient. As the PEG molecular mass increases from 400 g·mol⁻¹ (Table 3) to 4600 g·mol⁻¹ (Table 5), the precision of the measured D_{21} values improves considerably, by about an order of magnitude. This behavior

can be understood by noting the corresponding increase in the molar refractive index increment with PEG molecular weight. Molar coupled flows of the heavier PEG fractions can therefore be measured more precisely by the refractive index detector used in the present study.

D_{12} is zero within the precision of the measurements for several of the more dilute solutions. At the higher Triton X-100 concentrations, the values of D_{12} indicate that PEG concentration gradients drive significant co-current coupled flows of Triton X-100. A convenient relative measure of the strength of this coupled diffusion is provided by the ratio D_{12}/D_{22} , which gives the number of moles of Triton X-100 transported per mole of PEG driven by its own concentration gradient. The values of

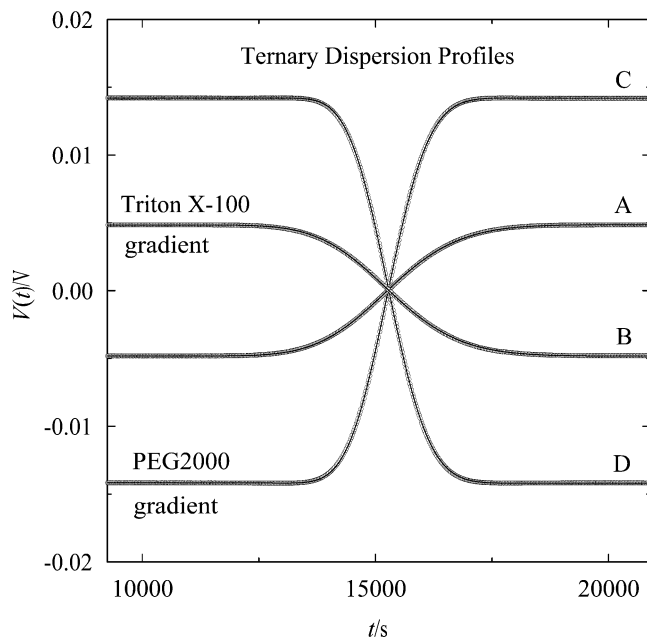


Figure 3. Ternary error-function profiles for aqueous Triton X-100 ($\bar{c}_1 = 5.00 \text{ mmol}\cdot\text{dm}^{-3}$) + PEG2000 ($\bar{c}_2 = 5.00 \text{ mol}\cdot\text{dm}^{-3}$) solutions: \circ , measured refractometer voltages; $-$, fitted voltages (eq 17). Profile A: $\Delta c_1 = 1.00$, $\Delta c_2 = 0.00$. Profile B: $\Delta c_1 = -1.00$, $\Delta c_2 = 0.00$. Profile C: $\Delta c_1 = 0.00$, $\Delta c_2 = 1.00$. Profile D: $\Delta c_1 = 0.00$, $\Delta c_2 = -1.00 \text{ mmol}\cdot\text{dm}^{-3}$.

D_{12}/D_{22} increase with concentration of Triton X-100 concentration and with the PEG molecular mass, reaching a maximum value of 2.2 at the composition $40.0 \text{ mmol}\cdot\text{dm}^{-3}$ Triton X-100 + $10.0 \text{ mmol}\cdot\text{dm}^{-3}$ PEG4600. Significantly stronger coupled diffusion has been reported³² for aqueous sodium dodecyl sulfate (NaDS) + PEG solutions, with up to 20 mol of NaDS co-transported per mole of diffusing PEG. According to the electrostatic mechanism suggested for the strongly coupled transport of the ionic surfactant, the co-current flux of NaDS micelles is driven by the electric field generated by the diffusion of mobile Na^+ counterions released when PEG segments bind to ionic micelles. An electrostatic mechanism for coupled transport cannot operate in solutions of Triton X-100 + PEG solutions, which might account for the smaller D_{12} values for this system.

Cross-coefficient D_{21} gives the coupled flux of PEG produced by a Triton X-100 concentration gradient. In this case D_{21}/D_{11} gives the number of moles of PEG co-transported per mole of Triton X-100 driven by its own concentration gradient. At the compositions used in the present study, a mole of diffusing Triton X-100 co-transported at most 0.2 mol of PEG. The minor coupled flows of PEG suggests that only small fractions of the total PEG molecules are bound to the Triton X-100 micelles, which is not unreasonable considering that the concentration of the Triton X-100 micelles is 25 to 200 times smaller than the concentration of the PEG molecules at the compositions used in the present study.

Conclusions

Moving-boundary Taylor experiments developed previously for binary solutions have been extended to measure ternary mutual diffusion coefficients for coupled diffusion in three-component solutions. In conventional Taylor experiments, pulse-injection initial conditions are used to generate Gaussian dispersion profiles at the outlet of the dispersion tube. Moving-boundary experiments employ step-function initial profiles that

evolve into error-function dispersion profiles. The main advantage of moving-boundary experiments is the absence of the strong dilution factor. As a result, ternary mutual diffusion coefficients, including cross coefficients for coupled diffusion, can be measured using relatively small initial concentration differences on the order of $\approx 0.001 \text{ mol}\cdot\text{dm}^{-3}$. This feature is useful in cases where the D_{ik} coefficients are strongly composition dependent and would otherwise vary significantly across the dispersion profiles or the dispersion profiles are broad as a result of slowly diffusing solutes, such as polymers or nonionic micelles.

Literature Cited

- (1) Tyrrell, H. J. V.; Harris, K. R. *Diffusion in Liquids*; Butterworths: London, 1984.
- (2) Erkey, C.; Akgerman, A. In *Measurement of the Transport Properties of Fluids*; Wakeham, W. A., Nagashima, A., Sengers, J. V., Eds.; Blackwell: London, 1991.
- (3) Dunlop, P. J.; Harris, K. R.; Young, D. J. *Physical Methods of Chemistry*, Vol. 1, Pt. IV; Wiley-Interscience: New York, 1992.
- (4) Alizadeh, A.; Nieto de Castro, C. A.; Wakeham, W. A. The theory of the Taylor dispersion technique for liquid diffusivity measurements. *Int. J. Thermophys.* **1980**, *1*, 243–284.
- (5) Pratt, K. C.; Wakeham, W. A. Mutual diffusion coefficient for binary mixtures of water and the isomers of propanol. *Proc. R. Soc. (London)* **1975**, *A342*, 401–419.
- (6) Chen, S. H.; Davis, H. T.; Evans, D. F. Tracer diffusion in polyatomic liquids. III. *J. Chem. Phys.* **1982**, *77*, 2540–2544.
- (7) Mathews, M. A.; Akgerman, A. Diffusion coefficients for binary alkane mixtures to 573 K and 3.5 MPa. *AIChE J.* **1987**, *33*, 881–885.
- (8) Price, W. E.; Trickett, K. A.; Harris, K. R. Association of caffeine in aqueous solution: effects on caffeine intradiffusion. *J. Chem. Soc. Faraday Trans. 1* **1989**, *85*, 3281–3288.
- (9) Erkey, C.; Alhamid, K. A.; Akgerman, A. Investigation of the effects of molecular association on diffusion in binary liquid mixtures at the infinite dilution limit. *J. Chem. Phys.* **1991**, *94*, 3867–3871.
- (10) Thiel, P.; Paschke, A.; Winkelmann, J. Determination of binary diffusion coefficients in liquid nonelectrolyte mixtures using the Taylor dispersion technique. *Ber. Bunsen-Ges. Phys. Chem.* **1992**, *96*, 750–753.
- (11) Harris, K. R.; Lam, H. H. Mutual-diffusion coefficients and viscosities for the water-2-methylpropan-2-ol system at 15 and 25 °C. *J. Chem. Soc., Faraday Trans.* **1995**, *91*, 4071–4077.
- (12) Barthel, J.; Gores, H. J.; Lohr, C. M.; Seidl, J. J. Taylor dispersion measurements at low electrolyte concentrations. I. Tetraalkylammonium perchlorate aqueous solutions. *J. Solution Chem.* **1996**, *25*, 921–935.
- (13) Funazukuri, T.; Nishio, M. Infinite dilution binary diffusion coefficients of C5-monoalcohols in water in the temperature range from 273.2 K to 353.2 K at 0.1 MPa. *J. Chem. Eng. Data* **1999**, *44*, 73–76.
- (14) Afzal Awan, M.; Dymond, J. Transport properties of nonelectrolyte liquid mixtures. XI. Mutual diffusion coefficients for toluene + *n*-hexane and toluene + acetonitrile at temperatures from 273 to 348 K and at pressures up to 25 MPa. *Int. J. Thermophys.* **2001**, *22*, 679–700.
- (15) Bueno, J. L.; Suarez, J. J.; Medina, I. Experimental binary diffusion coefficients of benzene and derivatives in supercritical carbon dioxide and their comparison with the values from the classic correlations. *Chem. Eng. Sci.* **2001**, *56*, 4309–4319.
- (16) Leaist, D. G. Ternary diffusion coefficients of 18-crown-6 ether–KCl–water by direct least-squares analysis of Taylor dispersion profiles. *J. Chem. Soc. Faraday Trans.* **1991**, *76*, 597–601.
- (17) Deng, Z.; Leaist, D. G. Ternary mutual diffusion coefficients of $\text{MgCl}_2 + \text{MgSO}_4 + \text{H}_2\text{O}$ and $\text{Na}_2\text{SO}_4 + \text{MgSO}_4 + \text{H}_2\text{O}$ from Taylor dispersion profiles. *Can. J. Chem.* **1991**, *69*, 1548–1553.
- (18) MacEwan, K.; Leaist, D. G. Incongruent diffusion (negative main diffusion coefficient) for a ternary mixed surfactant system. *J. Phys. Chem. B* **2002**, *106*, 10296–10300.
- (19) Leaist, D. G. Boltzmann transformation of Taylor dispersion profiles to measure concentration dependent diffusion coefficients. *Ber. Bunsen-Ges. Phys. Chem.* **1991**, *95*, 113–117.
- (20) MacEwan, K.; Leaist, D. G. Quaternary mutual diffusion coefficients for aqueous solutions of a cationic-anionic mixed surfactant from moments analysis of Taylor dispersion profiles. *Phys. Chem. Chem. Phys.* **2003**, *5*, 3951–3958.
- (21) Leaist, D. G.; Hao, L. Simultaneous measurement of mutual diffusion and intradiffusion by Taylor dispersion. *J. Phys. Chem.* **1994**, *98*, 4702–4706.

- (22) Clark, S.; Konermann, L. Diffusion measurements by electrospray mass spectrometry for studying solution-phase noncovalent interactions. *J. Am. Soc. Mass Spectrom.* **2003**, *14*, 430–441.
- (23) Leaist, D. G.; Hao, L. Gravitational stability of Taylor dispersion profiles. Revised diffusion coefficients for barium chloride–potassium chloride–water. *J. Phys. Chem.* **1993**, *97*, 1464–1469.
- (24) Miller, D. G.; Vitagliano, V. Experimental test of McDougall's theory for the onset of convective instabilities in isothermal ternary systems. *J. Phys. Chem.* **1986**, *90*, 1706–1717.
- (25) Robinson, R. A.; Stokes, R. H. *Electrolyte Solutions*, 2nd ed.; Butterworths: London, 1959.
- (26) Haase, R.; Siry, M. Diffusion in the critical separation region of binary liquid systems. *Z. Phys. Chem., N. F.* **1968**, *57*, 56–73.
- (27) Leaist, D. G. Binary diffusion of micellar electrolytes. *J. Colloid Interface Sci.* **1986**, *111*, 230–240.
- (28) Deng, Z.; Lu, H.; Leaist, D. G. Mutual diffusion coefficients and resistance coefficients of sodium alkanolate surfactant. *J. Chem. Eng. Data* **1996**, *41*, 214–217.
- (29) Leaist, D. G. A moving boundary technique for the measurement of diffusion in liquids. *J. Solution Chem.* **1991**, *20*, 187–197.
- (30) Dunlop, P. J. Diffusion and frictional coefficients for two concentrated compositions of the system water–mannitol–sodium chloride at 25 °C. *J. Phys. Chem.* **1965**, *69*, 4276–4283.
- (31) Ellerton, H. D.; Reinfelds, G.; Mulcahy, D.; Dunlop, P. J. The mutual frictional coefficients of several amino acids in aqueous solution at 25 °C. *J. Phys. Chem.* **1964**, *68*, 403–408.
- (32) Halvorsen, H.; Leaist, D. G. An electrostatic mechanism for the coupled diffusion of polymer molecules and ionic micelles. *Phys. Chem. Chem. Phys.* **2004**, *6*, 3515–3523.
- (33) Taylor, G. Dispersion of soluble matter in solvent flowing through a tube. *Proc. R. Soc. A (London)* **1953**, *219*, 186–203.
- (34) Grossmann, T.; Winkelmann, J. Ternary diffusion coefficients of glycerol + acetone + water by Taylor dispersion measurements at 298.15 K. *J. Chem. Eng. Data* **2005**, *50*, 396–403.
- (35) Qiao, L.; Easteal, A. J. The interaction between Triton X series surfactants and poly(ethylene glycol) in aqueous solutions. *Colloid Polym. Sci.* **1998**, *276*, 313–320.
- (36) Moulik, S. P.; Gupta, S. Das, A. R. Hydration studies on some polyhydroxy non-electrolytes and non-ionic surfactants. *Can. J. Chem.* **1989**, *67*, 356–363.

Received for review August 22, 2006. Accepted December 17, 2006. Acknowledgment is made to the Natural Sciences and Engineering Research Council for the financial support of this work.

JE0603731